Thermal Performance Prediction of the TMT Telescope Structure

Myung Cho[*1], Andrew Corredor[2], Konstantinos Vogiatzis[3], George Angeli[3]

[1]GSMT Program Office, National Optical Astronomy Observatory
950 N. Cherry Ave., Tucson, AZ 85719
[2]Aerospace and Mechanical Engineering Department, University of Arizona, Tucson, AZ 85721
[3]TMT Project Office, California Institute of Technology, Pasadena, CA 91125

ABSTRACT

Thermal analysis for the Thirty Meter Telescope (TMT) structure was performed using finite element analysis in ANSYS and I-DEAS. In the thermal analysis, the telescope structural parts with simplified optical assembly systems were modeled for various thermal conditions including air convections, conductions, heat flux loadings, and radiations. Thermal responses of the TMT telescope structure were predicted and the temperature distributions of the optical assembly systems were calculated under sample thermal loading conditions. The thermo-elastic analysis was made to obtain the thermal deformation based on the resulting temperature distributions. The line of sight calculation was made using the thermally induced structural deformations. The goal of this thermal analysis is to establish thermal models by the FEA programs to simulate for an adequate thermal environment. These thermal models can be utilized for estimating the thermal responses of the TMT structure. Thermal performance prediction of the TMT structure will be able to guide us to control and maintain the system from the "seeing" effects.

Keywords: telescope structure thermal analysis, temperature distributions, thermo-elastic analysis, merit function

1. INTRODUCTION

The Thirty Meter Telescope Observatory Corporation has recently announced that Mauna Kea as the preferred site for the TMT after careful evaluation and comparison among several outstanding candidate sites. For large ground-based telescopes, balancing the performance between wind buffeting and mirror and dome seeing has always been one of the challenging requirements to fulfill scientific goals. A two-year environmental measurement of the TMT baseline site[7] and Computational Fluid Dynamics (CFD) techniques provide the thermal environment parameters surrounding the TMT structure. For thermal finite element models, the environmental record and CFD predictions provide expected flow fields and thermal boundary conditions in terms of ambient air profiles, convection coefficients, heat fluxes, and radiation properties. These parameters were implemented to predict thermal responses and thermal deformations of the TMT structure.

Thermal analysis for the Thirty Meter Telescope Structure was performed using finite element analysis in ANSYS. In such analysis, the entire telescope structure was modeled and analyzed under different thermal loads. The temperature distribution on the model was calculated using predetermined heat loads. The present case study was performed in order to predict the thermal responses of the telescope structure in two different spatial configurations; horizon pointing configuration (Service/Maintenance as a Daytime mode) and observation configuration (Zenith Angle = 32º as a Nighttime mode).

The telescope model analyzed in this report incorporates the entire elevation structure, the azimuth structure, the foundation pier structure and the nasmyth platforms as shown below in Figure 1. The present model was developed based on the dimensions and physical properties specified in the latest revision of the telescope finite element structure created by *Empire Dynamic Structures, Ltd.* The major geometric parameters of the telescope model are listed in Table 1; a more detailed description of the model is given in the telescope finite element summary (FEM Revision 11.3-10).

* mcho@noao.edu; phone 1 520 318-8544; fax 1 520 318-8424; www.noao.edu

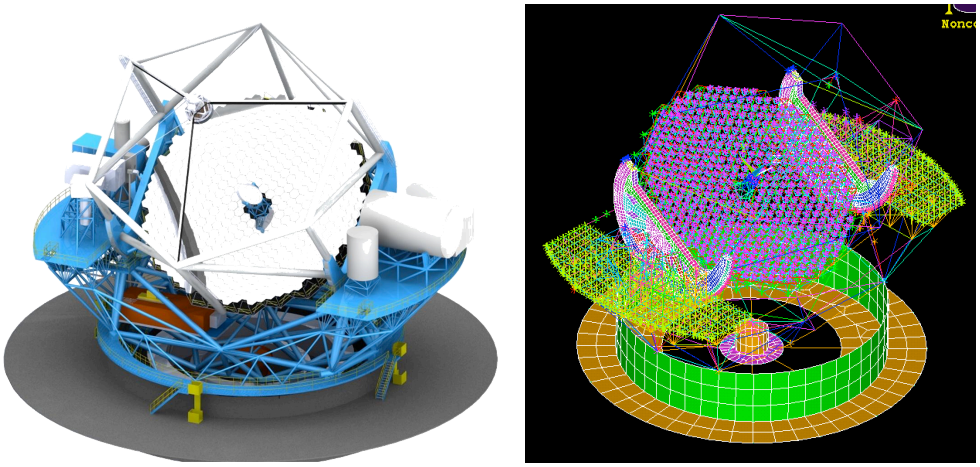

Fig. 1. Telescope Structure CAD model and finite element model at Zenith angle of 30 degrees.

Table 1: Major geometric parameters of the telescope

Major Geometric Parameters	
M1 Cell Depth	2.0 m
Elevation Journal Spacing (Half)	15.25 m
Elevation Journal Centerline Radius	10.75 m
Elevation Journal Depth (ex. stiffening part)	1.75 m
Top-End Hexagonal Ring Elevation	14.5 m
M2 CG Elevation	24.251 m
M3 CG Elevation	-0.84m
Azimuth Track Radius	17.64 m
Top of Azimuth Track Elevation	-19.0 m
Nasmyth Platform Half Length	15.0 m
Nasmyth Platform Outer Edge Radius	27.6 m
Nasmyth Platform Elevation (ex. deck)	-7.4 m

In addition to the geometric parameters, the thermal properties of steel and concrete were listed in Table 2 and used in the thermal analysis.

Table 2: Thermal properties of Steel and Concrete

Steel Thermal Properties	
Thermal conductivity	16.2 W/mºC
Specific heat	500 J/kgºC
Density	Specified in FEM Revision 11.3-10
Concrete Thermal Properties	
Thermal conductivity	1.2 W/mºC
Specific heat	840 J/kgºC
Density	Specified in FEM Revision 11.3-10

Moreover, the instruments located on both nasmyth platforms were modeled in order to analyze the thermal effects on the structure due to the heat dissipated by them in the form of radiation. For the purpose of this study, the instruments were assumed to have the physical and thermal properties of steel; an exploded view of the instruments and their corresponding supports is shown in Figure 2.

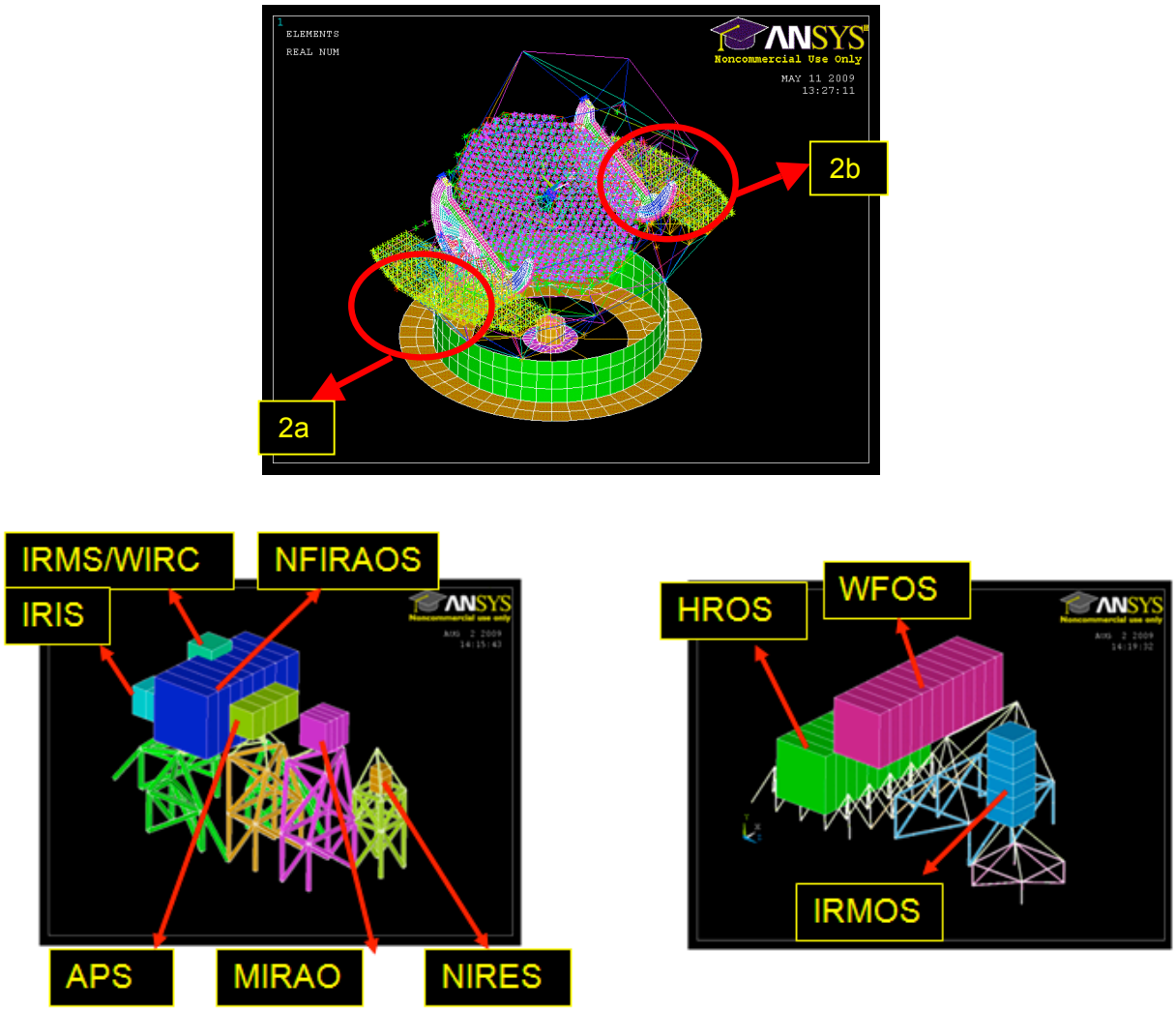

Fig. 2. Instruments on Nasmyth platforms; (2a) instruments on left Nasmyth platform (-X axis), (2b) Instruments on right (+X axis),

The thermal environment of the telescope is shown in Figure 3. The boundary conditions on the telescope include the heat dissipated from each instrument as well as the heat dissipated from secondary and tertiary mirrors, convection of air on the telescope structure's surfaces excluding the foundation pier, radiation exchange from surface to surface, and radiation losses to the environment. The basic heat transfer is described with conduction, convection and radiation. Moreover, it is observed that Fourier's equation is satisfied inside every element in the structure:

$$\frac{\partial T}{\partial t} = \alpha \nabla^2 T = \alpha \left(\frac{\partial^2 T}{\partial x^2} + \frac{\partial^2 T}{\partial y^2} + \frac{\partial^2 T}{\partial z^2} \right) \tag{1}$$

Where T is the structure's temperature, t is time and, α is the thermal diffusivity given by

$$\alpha = \frac{k}{\rho C_p} \tag{2}$$

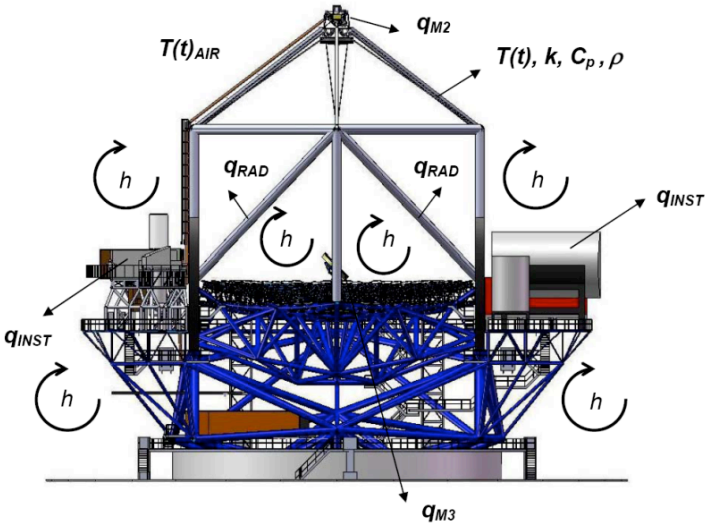

Fig. 3. Thermal Environment of the Telescope

Where

h: Heat transfer coefficient (varies depending on location)
q_{INST}: Instrument heat dissipation
q_{M2}: M2 Heat dissipation
q_{M3}: M3 Heat dissipation
q_{RAD}: Radiation losses
T(t): Air Temperature
T(t): Surface temperature

By using finite element methods, detailed analyses have been performed on the telescope. Current thermal FE models do not include heat transfers due to the heat dissipation at M1, q_{M1} , and radiation losses at the top-end, q_{RAD_TE}, but they will be included in next revision. The thermal response of the finite element model was obtained and it was plotted for both observation and maintenance/service configurations.

2. THERMAL ANALYSIS

2.1.1 Thermal Loads and Boundary Conditions

In order to investigate the thermal response of the telescope, reasonably well defined telescope operation boundary conditions were assumed for the entire structure model. Such conditions were air convection on the telescope's surfaces, heat dissipation from the instruments as well as the secondary and tertiary mirrors, radiation exchange from surface to surface and radiation losses to the environment. Furthermore, different analyses have been conducted in order to clarify the thermal results. In this report, the following analyses were performed and the results were discussed:

1. Maintenance/ Service Configuration:
- Case A: Conduction Analysis (Heat generation)
- Case B: Convection Analysis (Air convection)
- Case C: Radiation Analysis
- Case D: Combined thermal loads (Air convection, Radiation, and conduction)

2. Observation Configuration:
   - Case A: Conduction Analysis (Heat generation)
   - Case B: Convection Analysis (Air convection)
   - Case C: Radiation Analysis
   - Case D: Combined thermal loads (Air convection, Radiation, and conduction)

2.1.2 Air temperature variation

Extensive CFD analyses have been performed to quantify air flows inside the enclosure. Moreover, some simulation schemes have been developed for the air temperature distribution around the telescope. In the present analyses, air temperature profiles obtained from CFD simulations are used for the air convection cases.

For the Maintenance/ Service Configuration, three temperature profiles are used for the entire telescope structure as depicted in Figures 4 (Daytime - 12 hour heat cycle). In Figures 5, ambient air temperature profiles at each of three sections shown in Figure 4. Furthermore, for the Observation configuration, the maximum air temperature difference relative to the temperature of the structure was 2.0 ºC during the nighttime 12 hour heat cycle as shown in Figure 6. This ambient air temperature profile recorded at every 2 minutes from CFD was applied on the telescope structures.

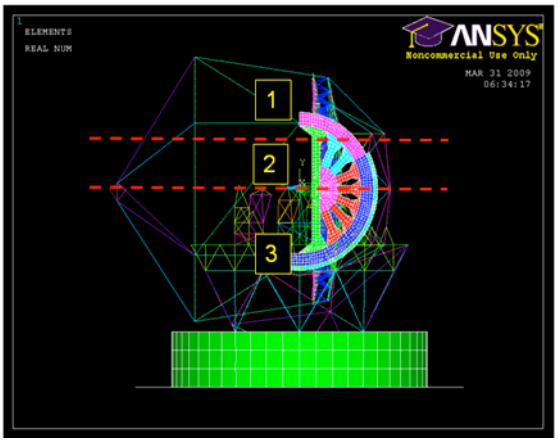

Fig. 4. Spatial variation of air temperature on telescope structure

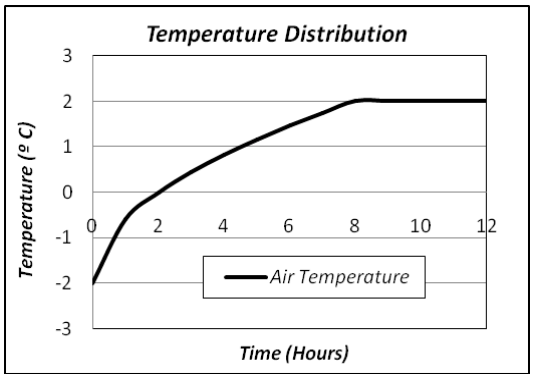

Fig.5.1. Air temperature profile for section 1 (See Fig. 4)

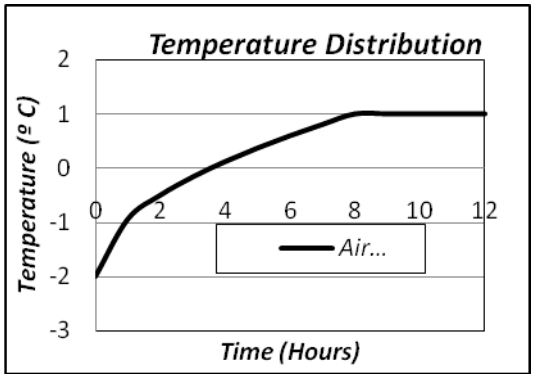

Fig. 5.2 Air temperature profile for section 2 (See Fig. 4)

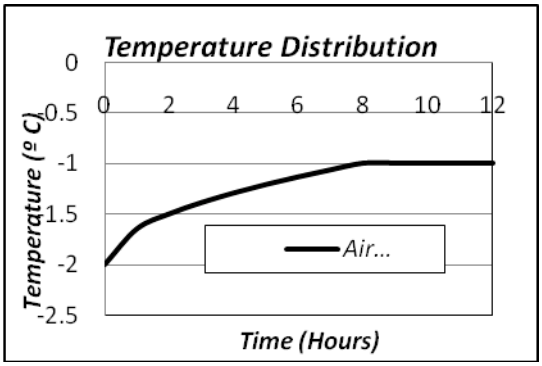

Fig. 5.3 Air temperature profile for section 3 in Fig. 4

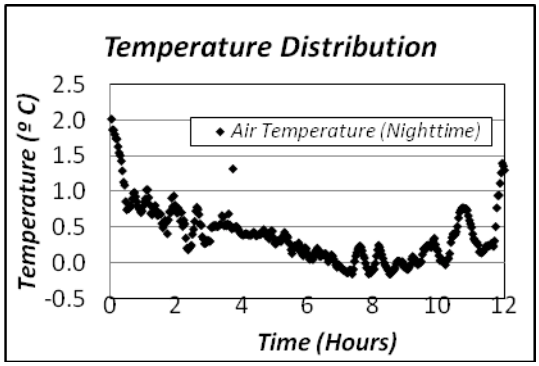

Fig.6. Air temperature variation for Nighttime mode

2.1.3 Conduction Analysis (Heat Dissipation)

The conduction effects on the telescope were determined by using the heat dissipated by the instruments located on the nasmyth platforms, and the heat dissipated by the secondary, tertiary mirrors, and laser facility for adaptive optics systems. The heat dissipated by each of these components is listed in Table 3. It should be noted that in both daytime and nighttime configurations, the heat flow values shown above were assumed to be constant for the duration of the heat cycle.

Table 3: Heat Dissipation for Daytime and nighttime configurations

Item Name	Shape /Qty.	Volume	Surface area	Nighttime Heat N AA	Nighttime Heat from Glyc	Daytime Heat Dumps D AA	Daytime Heat Dumps from Glyc
NFIRAOS optical bench(4*4*8)	Box	Space envelope drawing	160.0	-1	0	-1	0
NFIRAOS electronics cabinet	1	3.7 (W) x 2 (H) x 0.9 (D)	25.1	0.2	0.4	0.2	0.4
IRMS/WIRC	Cylinder	2 (Dia.) x 4 (H)	31.4	0.1		0.1	
WIRC electronics cabinet	3	1.8 (W) x 2 (H) x 0.9 (D)	14.0		0.09		0.09
IRIS	Cylinder	2 (Dia.) x 4 (H)	31.4	0.1		0.1	
IRIS electronics cabinet	4	2.4 (W) x 2 (H) x 0.9 (D)	17.5		0.25		0.25
NIRES-B/NIRES-R	Cylinder	1 (Dia.) x 1.5 (H)	6.3	0.1		0.1	
NIRES electronics cabinet	3	1.8 (W) x 2 (H) x 0.9 (D)	14.0		0.075		0.075
APS	Box	3 (W) x 1 (H) x 4 (D)	38.0	0.1		0.1	
APS electronics cabinet	2	1.2 (W) x 1.2 (H) x 0.9 (D)	7.2		0.25		0.25
MIRAO	Box	1.3 (W) x 2.85 (H) x 2.2 (D)	25.7	0.1		0.1	
MIRES	Cylinder	1.5 (Dia.) x 3.8 (H)	21.4	0.1	0.075	0.1	0.075
MIRAO/MIRES electronics cabinet	3	1.8 (W) x 2 (H) x 0.9 (D)	14.0		0.1		0.1
WFOS	Cylinder	7 (Dia.) x 11.7 (D)	334.1	0.1		0.1	
WFOS electronics cabinet	3	1.8 (W) x 2 (H) x 0.9 (D)	14.0		0.3		0.3
HROS	Box	11 (W) x 4 (H) x 10 (D)	388.0	0.1		0.1	
HROS electronics cabinet	3	1.8 (W) x 2 (H) x 0.9 (D)	14.0		0.75		0.75
HROS enclosure cooling	Box	2 (W) x 2 (H) x 2 (D)	24.0		0.25		0.25
IRMOS	Cylinder	4 (Dia.) x 5.9 (D)	99.2	0.1		0.1	
IRMOS meat locker	Box	1 (W) x 2 (H) x 2 (D)	16.0		0.25		0.25
IRMOS electronics cabinet	7	4.3 (W) x 2 (H) x 0.9 (D)	28.5		0.75		0.75
M2 Cell				0.25	0.25	0.25	0.25
M2 Cell control				0.3	0.3	0.3	0.3
M2 Hexapod				0.21	0.21	0.21	0.21
M2 Hexapod control				0.3	0.3	0.3	0.3
M3 Cell				0.25	0.25	0.25	0.25
M3 Cell control				0.3	0.3	0.3	0.3
M3 Positioner				0.33	0.33	0.33	0.33
M3 Positioner control				0.3	0.3	0.3	0.3
LGF/LSE (AZ in -Y)	Box	Space envelope drawing		0.2	0.48	0	0.48
LGF/LSE (AZ in +Y)	Box	Space envelope drawing		0.2	0.48	0	0.48
LGF/LSE top end and BTO (with control)				0	0.13	0	0.13

2.2 Finite Element Models

In order to calculate the temperature distribution of the Telescope structure, a finite element thermal model was generated using ANSYS. The beams, trusses, and supports of the telescope were modeled using thermal conductive elements (LINK33), and the C-Rings were modeled using thermal shell elements (SHELL 57). In addition to these elements, thermal convective (LINK32) and radiative (LINK31) elements were created in order to perform the convection and radiation analysis, respectively. Such link elements simplify the complexity of the analysis by allowing the input of surface convective and radiative areas, and emissivity coefficients without having to create solid models for the convective and radiative analyses. Additionally, a superelement (MATRIX50) was used in order to perform the radiation analysis between surfaces (C-Rings). The finite element model used in this analysis is shown in Figure 7. By conducting a thermal analysis in ANSYS, the temperature distribution for the different cases described previously was calculated.

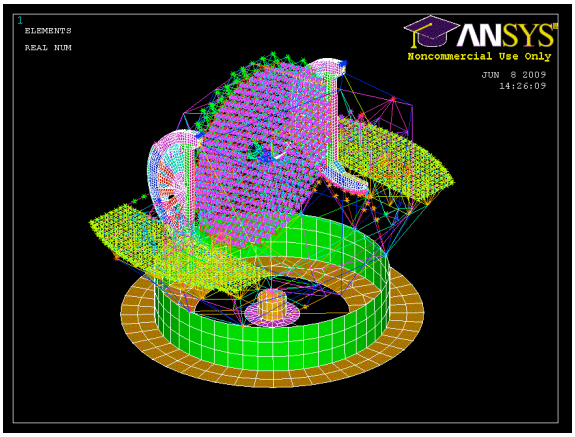

Fig. 7. Telescope Structure Finite Element (90º Zenith Angle)

2.3 Thermal Analysis Results - Daytime Configuration

2.3.1 Case 1A: Conduction Analysis

In case 1A, the heat dissipation values from Table 3 were applied to each of the instruments on the telescope model at a zenith angle of 90 degrees. From the FE result, the maximum and minimum temperature responses obtained were 4.47 ºC and -1.49 ºC, respectively (Figure 8.1). From the contour plot, it is observed that the conduction effect is very small in a global context; the effect of conduction is more local and is only noticeable in regions near the instruments which are the regions of application of the heat loads (Figure 8.2).

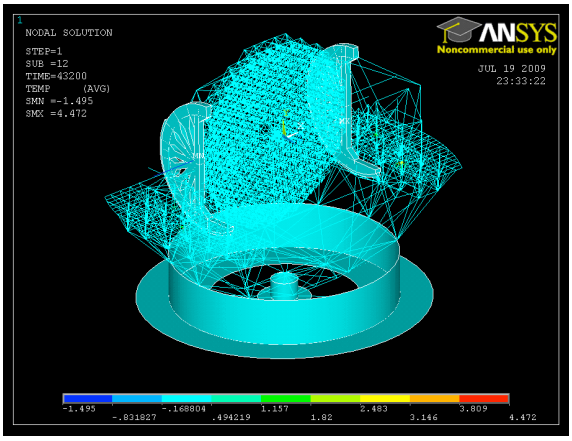

Fig. 8.1. Temperature Distribution (Case 1A - Conduction)

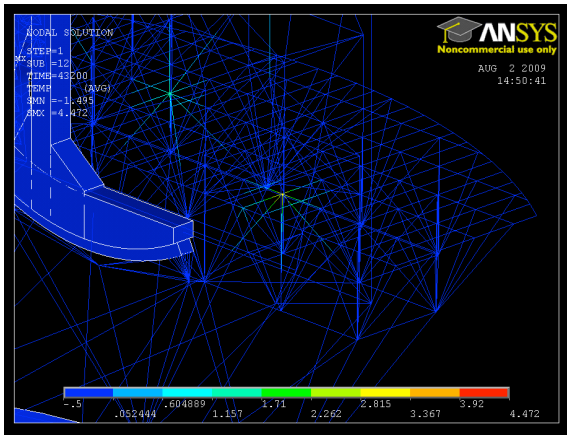

Fig. 8.2. Temperature Distribution (Conduction local effect)

2.3.2 Case 1B: Convection Analysis

In case 1B, air convection was applied on the Telescope's surfaces with different heat transfer coefficients depending on the spatial location. For the primary mirror support system (M1SS), the heat transfer coefficient was assumed to vary from 1 W/m^2 ºC to 5 W/m^2 ºC, as depicted in Figure 9.

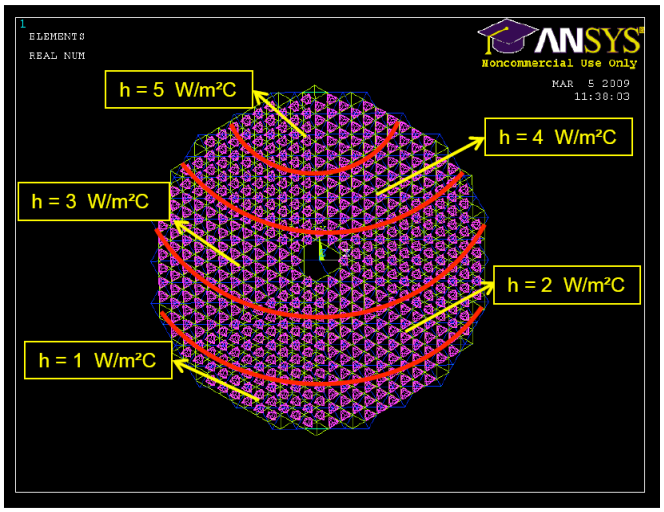

Fig. 9. Spatial distribution of heat transfer coefficient on M1SS

All the other components in the structure were assumed to have a heat transfer coefficient of 3 W/m^{2}ºC. The air temperature profile described previously and these heat transfer coefficients were used to obtain the temperature response for the telescope's daytime configuration. The maximum and minimum temperature responses obtained for the telescope from the analysis were 2 ºC and -1.02 ºC, respectively (Figure 10). Moreover, the temperatures obtained for M1SS were 2 ºC as a maximum and -1 ºC as a minimum (Figure 11).

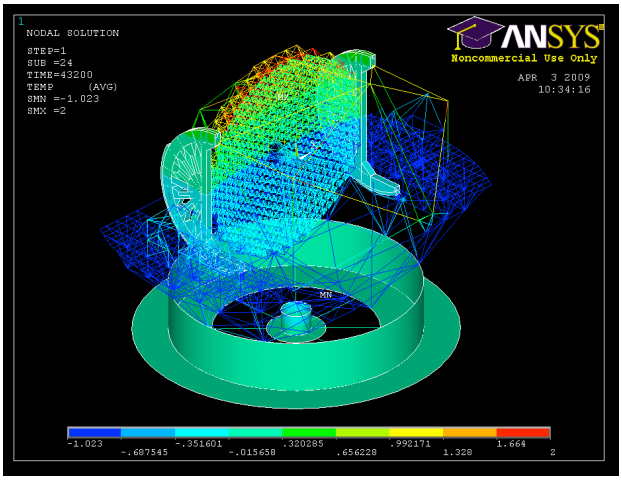

Fig. 10. Temperature Distribution (Case 1B - Convection)

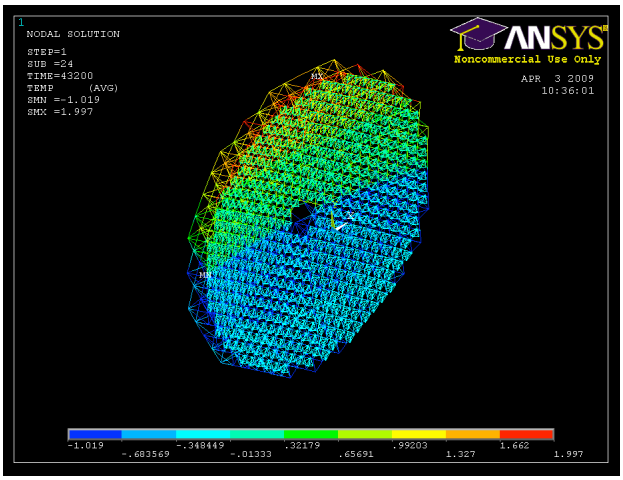

Fig. 11. Temperature Distribution M1SS (Case 1B – Convection)

2.3.3 Case 1C: Radiation Analysis

In the present case, a constant background temperature was utilized for the radiation analysis (Figure 12). This is a sample case to simulate the telescope structure inside enclosure. In addition to this temperature, emissivity values were assigned to every component on the telescope; the following are the emissivity coefficients used in the analysis:

- M1 Support Structure (M1SS): Front ε = 0.6, Back ε = 1.0, Intermediate ε = 0.8
- Structure above M1, ε = 0.4
- Structure behind M1SS, ε = 1.0
- Platform and Platform Supports, ε = 0.8
- Instrument Supports, ε = 1.0
- Instruments, ε = 0.4
- No Radiation Loads were applied on the concrete piers

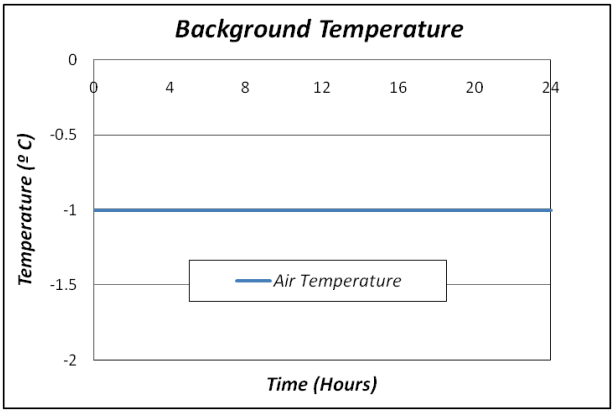

Fig. 12. Background temperature profile

The temperature distribution for the daytime configuration of the telescope was obtained and it was plotted. The peak temperature response obtained was 0.003 ºC and the minimum response was -1 ºC (Figure 13). Moreover, the temperature responses obtained for M1SS were calculated to be -0.195 ºC as the maximum and for the minimum a value of -1 ºC was obtained (Figure 14).

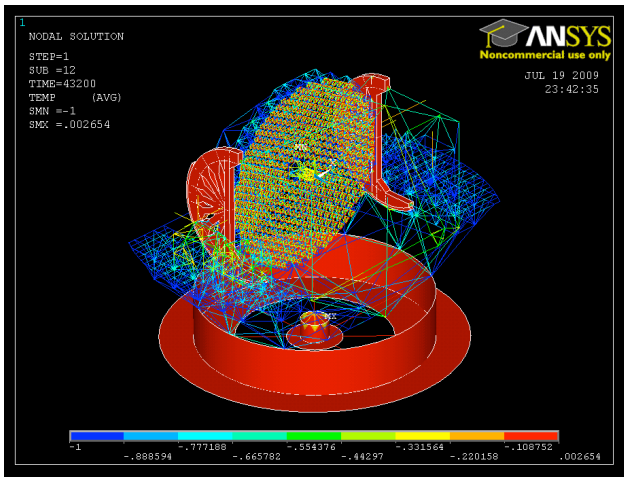

Fig.13. Temperature distribution (Case 1C- Radiation)

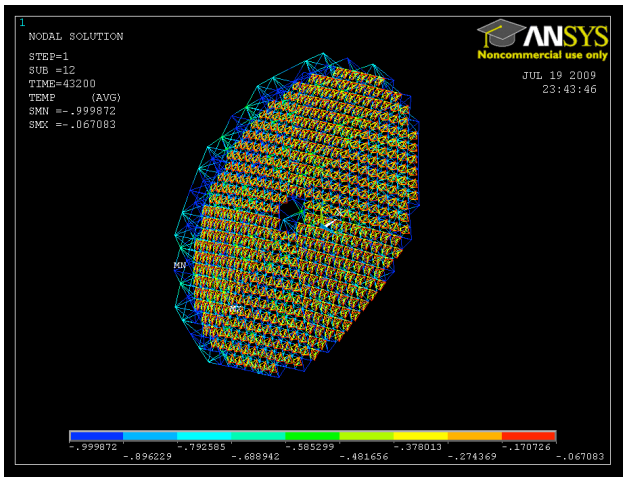

Fig. 14. Temperature Distribution M1SS (Case 1C - Radiation)

2.3.4 Case 1D: Combined Thermal Loads

The temperature distribution of the telescope at a zenith angle of 90º was calculated by combining the thermal loads used in the previous cases (air convection and radiation analyses). The temperature response obtained for the telescope

structure at the end of the first 12 hours was 2 ºC and the minimum temperature was -1 ºC. Moreover, the maximum and minimum temperatures obtained for M1SS at this time were 0.73 ºC and -1 ºC, respectively. The temperature distribution for both the telescope and M1SS are shown Figures 15 and 16.

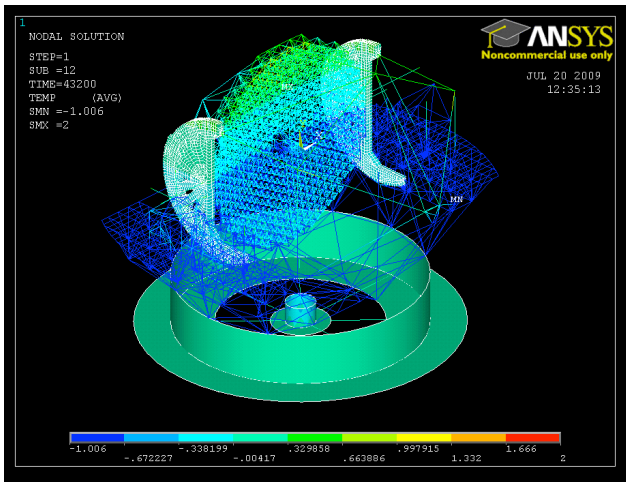

Fig. 15. Temperature distribution (Combined thermal loads)

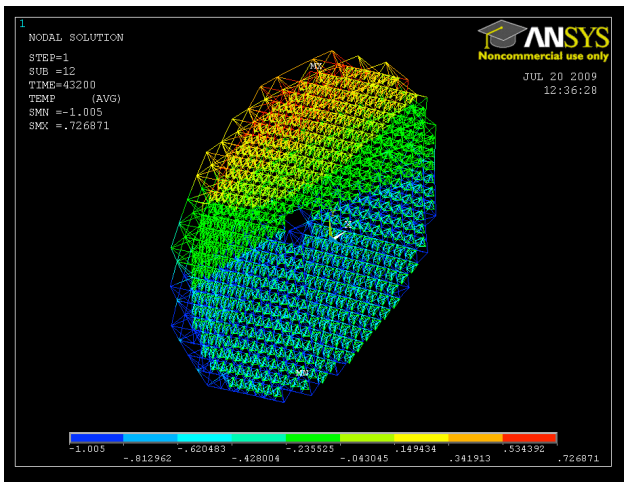

Fig. 16. Temperature distribution on M1SS

2.4 Results Nighttime Configuration

2.4.1 Case 2A: Conduction Analysis

In case 2A, the heat dissipation values from Table 3 were applied to each of the instruments on the telescope model at a zenith angle of 32º degrees. From the FE result, the maximum and minimum temperature responses obtained were 4.33ºC and -1.49 ºC, respectively (Figure 17.1). From the contour plot, it is observed that the conduction effect is very small in a global context; the effect of conduction is more local and is only noticeable in regions near the instruments which are the regions of application of the heat loads (Figure 17.2).

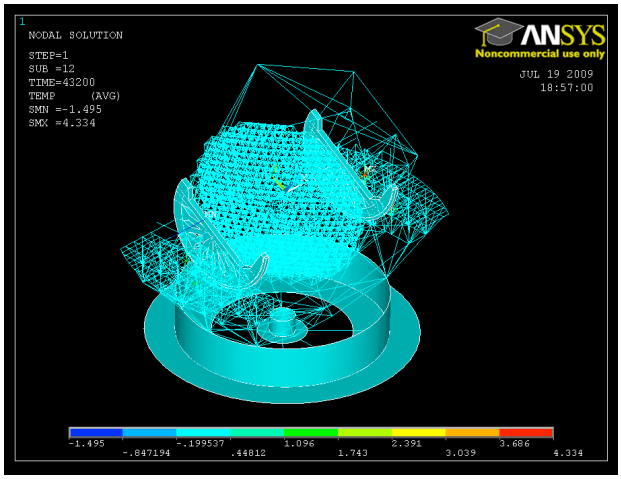

Fig. 17.1. Temperature Distribution (Case 2A - Conduction)

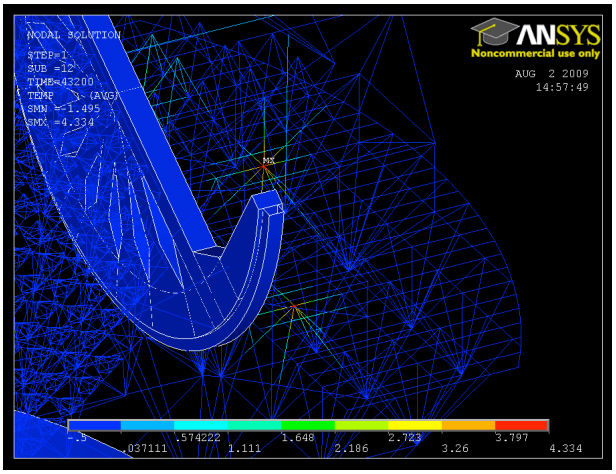

Fig. 17.2. Temperature Distribution (Conduction local effect)

2.4.2 Case 2B: Convection Analysis

In case 2B, air convection was applied on the Telescope's surfaces with different heat transfer coefficients depending on the spatial location. For the primary mirror support system (M1SS) the heat transfer coefficient varied from 1 W/m^2 ºC to 5 W/m^2 ºC as shown in Figure 9. All the other components in the structure were assumed to have a heat transfer coefficient of 3 W/m^{2}ºC. The air temperature profile shown in Figure 6 and these heat transfer coefficients were used to obtain the temperature response for the telescope's nighttime configuration. The maximum and minimum temperature responses obtained for the telescope from the analysis at the end of the night were 1.293ºC and -ºC, respectively (Figure 18). Moreover, the temperatures obtained for M1SS were ºC as a maximum and ºC as a minimum (Figure 19).

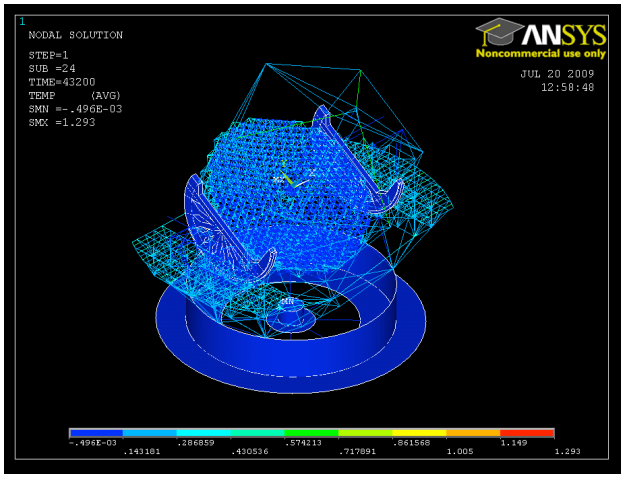

Fig. 18. Temperature distribution (Case 2B - Convection)

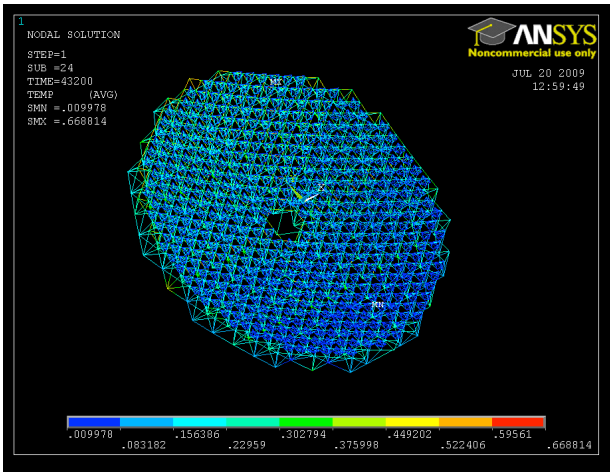

Fig. 19. Temperature distribution M1SS (Case 2B - Convection)

2.4.3 Case 2C: Radiation Analysis

In the present case, a constant background temperature was utilized for the radiation analysis as shown in Figure 12. In addition to this temperature, emissivity values were assigned to every component on the telescope; the following are the emissivity coefficients used in the analysis:

- M1 Support Structure (M1SS): Front ε = 0.6, Back ε = 1.0, Intermediate ε = 0.8
- Structure above M1, ε = 0.4
- Structure behind M1SS, ε = 1.0
- Platform and Platform Supports, ε = 0.8
- Instrument Supports, ε = 1.0
- Instruments, ε = 0.4
- No Radiation Loads were applied on the concrete piers

The temperature distribution for the nighttime configuration of the telescope was obtained and it was plotted. The peak temperature response obtained was 0.0027ºC and the minimum response was -1 ºC (Figure 20). Moreover, the temperature responses obtained for M1SS were calculated to be -0.22 ºC as the maximum and for the minimum a value of -1 ºC was obtained (Figure 21).

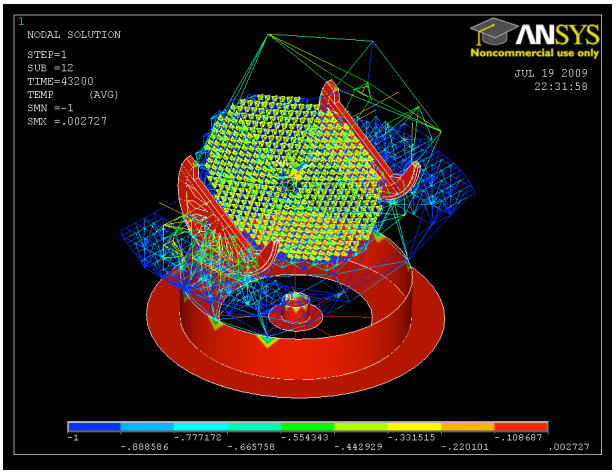

Fig.20. Temperature distribution (Case 2C - Radiation)

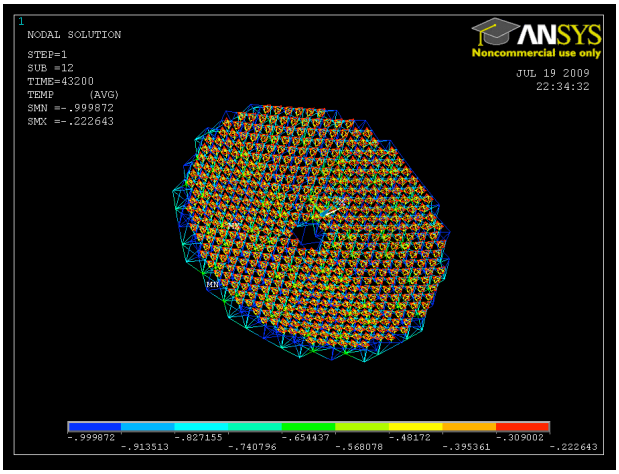

Fig. 21. Temperature distribution M1SS (Case 2C - Radiation)

2.4.4 Case 2D: Combined Thermal Loads

The temperature distribution of the telescope at a zenith angle of 32º was calculated by combining the thermal loads used in the previous cases (air convection and radiation analyses). The temperature response obtained for the telescope structure at the end of the night was 0.0936 ºC and the minimum temperature was -1 ºC. Moreover, the maximum and minimum temperatures obtained for M1SS at this time were -0.013ºC and -0.78ºC, respectively. The temperature distribution for both the telescope and M1SS are shown Figures 22 and 23.

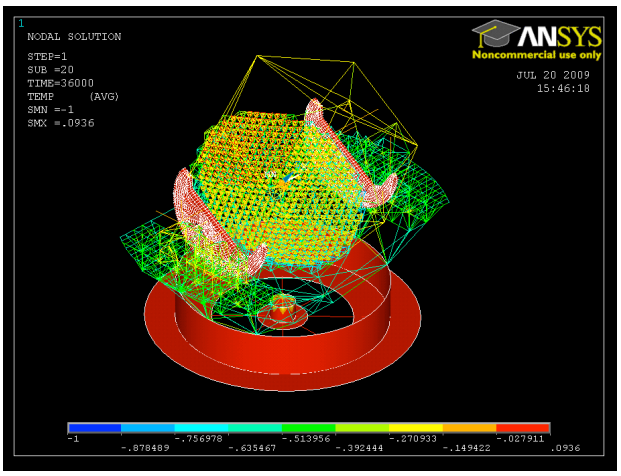

Fig. 22. Temperature distribution (Combined thermal loads)

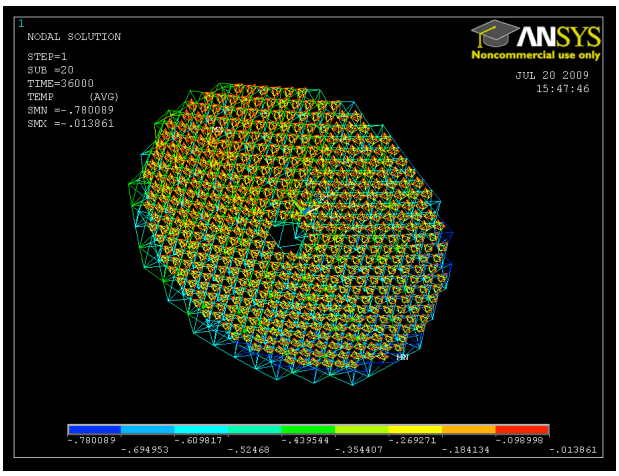

Fig. 23. Temperature distribution M1SS (Combined thermal loads)

2.5 Thermo-elastic Analysis

The thermal deformation of the telescope was calculated for both the maintenance/service configuration and the observation configuration using the thermal responses from the peak temperatures during these 12 hour heat cycles.
From the thermal analyses performed in cases 1D and 2D, the nodal temperature at 12 hours was applied to the horizon-pointing telescope model in order to perform the thermo-elastic analysis. Similarly, the nodal temperature at 10 hours was used as the heat load in order to obtain the thermal deformation of the telescope on its observation configuration.

For the thermo-elastic analysis, the structural finite element model created by *Empire Dynamic Structures, Ltd.* was utilized. The displacements on the x, y, and z directions were constrained at the concrete pier for both daytime and nighttime configurations as shown in Figures 24 and 25.

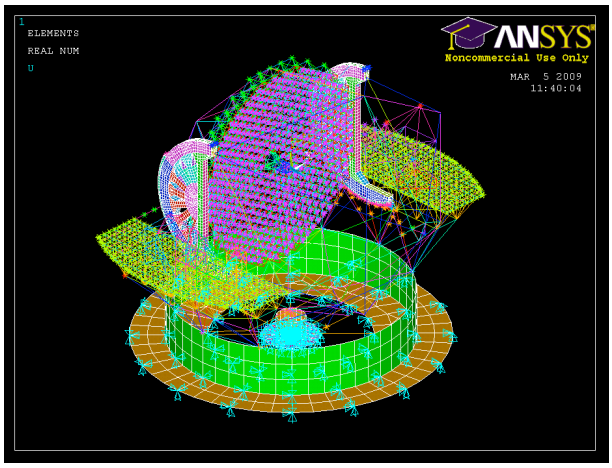

Fig. 24. Boundary Conditions on telescope structure (ZA = 90º)

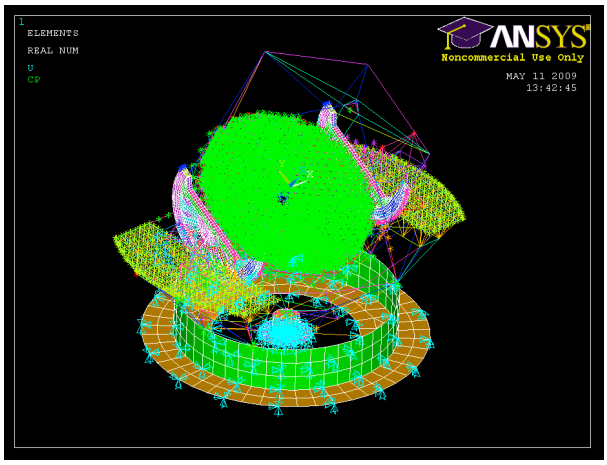

Fig. 25. Boundary Conditions on telescope structure (ZA = 32º)

2.5.1 Thermal Deformation (Daytime Configuration)

The thermal deformation of the telescope at a zenith angle of 90º was calculated using the temperature response at 12 hours from the combined loads case. The maximum displacement obtained for the telescope structure on the z direction was 306 µm and the minimum displacement was -185 µm. Moreover, the maximum and minimum displacements obtained for M1SS in the same direction were 159 µm and -45.8 µm, respectively. The thermal deformation for both the telescope and M1SS are shown Figures 26 and 27.

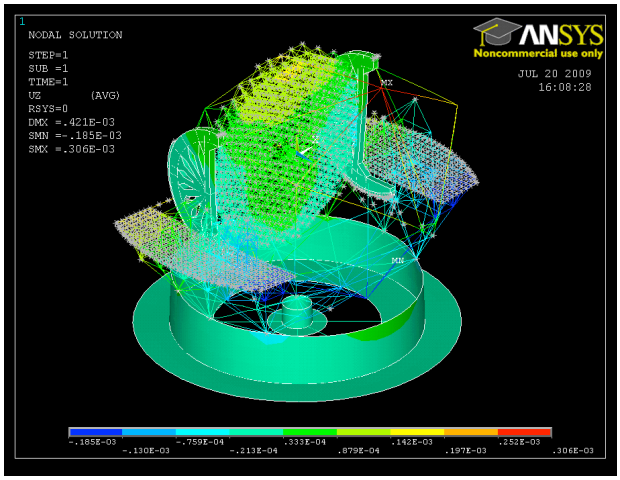

Fig. 26. Thermal deformation of the structure at t = 12 hrs

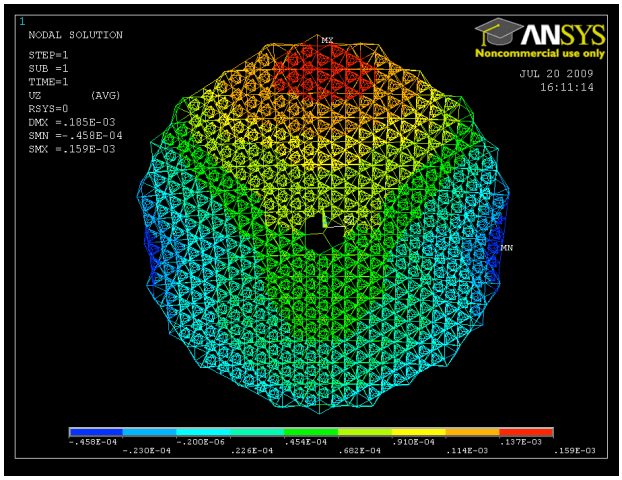

Fig. 27. Thermal deformation of the M1SS at t = 12 hrs

2.5.2 Thermal Deformation (Nighttime Configuration)

The thermal deformation of the telescope at a zenith angle of 32º was calculated using the temperature response at 10 hours from the combined loads case. The maximum displacement obtained for the telescope structure on the z direction was 86.0 µm and the minimum displacement was -97.7 µm. Moreover, the maximum and minimum displacements obtained for M1SS in the z direction were 55.9 µm and -56.5 µm, respectively. The thermal deformation for both the

telescope and M1SS are shown in the following Figures 28 and 29. Merit function (MF) which calculates the surface maps after repositioning the optics based on a best fit of M1 segment deformations. MF also calculates the stroke motion of M1 actuators required to maintain the optical alignment. Uncorrected M1 segment OPD map and actuator stroke requirement are shown in Figure 30.

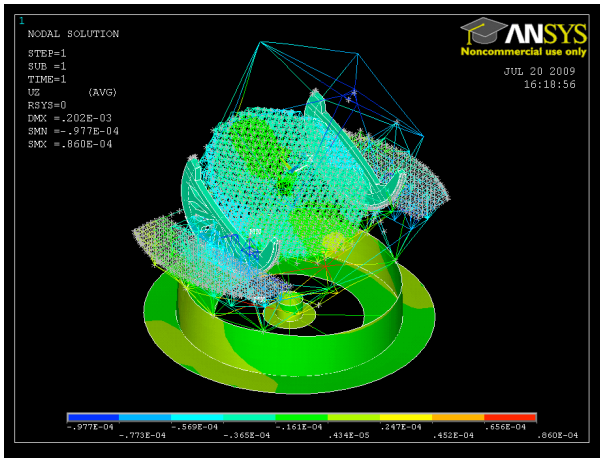

Fig. 28. Thermal deformation of the structure at t = 10 hrs

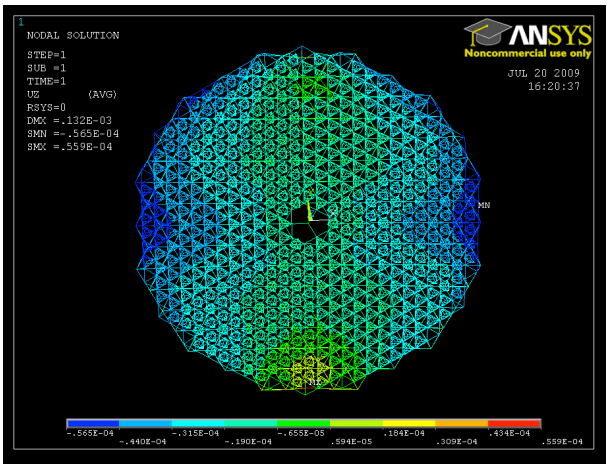

Fig. 29. Thermal deformation of the M1SS at t = 10 hrs

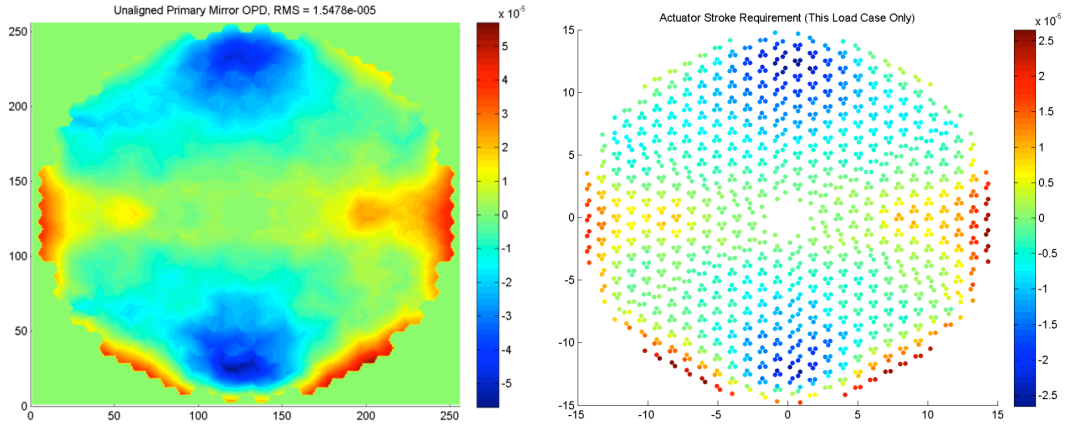

Fig. 30. Uncorrected OPD map and stroke motion for the M1segments from Merit function at t = 10 hrs. The OPD map shows a surface RMS of 15 microns, and actuator requirement shows a maximum actuator stroke of +/- 25 microns.

SUMMARY AND CONLUSIONS

In order to calculate the temperature distribution of the thirty meter telescope structure, thermal finite element analysis was performed using ANSYS. From the thermal responses obtained for the telescope, it was noticed that the conduction effects are only observable at a local level. Moreover, it was seen that the most dominant modes of heat transfer on the model were convection and radiation.

From the combined thermal analyses performed on the telescope, the maximum and minimum temperatures obtained for the daytime configuration at 12 hours were 2 ºC and -1 ºC, respectively. Additionally, the maximum and minimum thermal displacements obtained in the z direction were 306 µm and -185 µm. Similarly, for the nighttime configuration the maximum temperature obtained was 0.094 ºC and the minimum was -1 ºC. The maximum and minimum thermal

displacements obtained in the z direction were 86.0 μm and -97.7 μm. Merit function predicts a maximum M1 segment actuator requirement of 25 microns to maintain the optical alignment.

ACKNOWLEDGMENTS

This research was carried out at the National Optical Astronomy Observatory, and was sponsored in part by the TMT. The authors gratefully acknowledge the support of the TMT partner institutions. They are the Association of Canadian Universities for Research in Astronomy (ACURA), the California Institute of Technology and the University of California. This work was supported as well by the Gordon and Betty Moore Foundation, the Canada Foundation for Innovation, the Ontario Ministry of Research and Innovation, the National Research Council of Canada, the Natural Sciences and Engineering Research Council of Canada, the British Columbia Knowledge Development Fund, the Association of Universities for Research in Astronomy (AURA) and the U.S. National Science Foundation.

The authors would like to acknowledge Virginia Ford, Curtis Baffes, Eric Williams, Larry Stepp, Eric Chauvin, Kei Szeto, Hugh Thompson, and Scott Roberts of the TMT Project for their review and helpful comments.

REFERENCES

[1] Mast, T. and Nelson, J., "TMT Image Size and Wavefront Error Budgets Volume 1 2, 3", TMT.OPT.TEC.07.001, (2007)

[2] Cho, M. and Corredor, A., "TMT M1 Segment Thermal Analysis", TMT.SEN.TEC.06.034.DRF01, December 12, (2006).

[3] Ponchione, R.J., Ponslet, E., Setoodeh, S., Stephens, V., Tubb, A. and Williams, E., "TMT M1 Segment Support Assembly (SSA) Preliminary Design Review (PDR)", IMTEC, TMT.OPT.PRE.07.056.REL01, October 24, (2007)

[4] Cho, M. and Corredor, A., "Thermal Analysis of TMT M1 Segment Assembly", TMT.SEN.TEC.08.021.DRF01, December 12, April, (2008).

[5] Cho, M. and Pootrakul, S., "Thermal Analysis of TMT Secondary Mirror Assembly and Tertiary Mirror Assembly," TMT.SEN.TEC.08.022.DRF01, April, (2008).

[6] Vogiatzis, K., "Advances in Aero-thermal Modeling for TMT", SPIE 7017-29, Marseille, France, (2008).

[7] Schöck, M., et al., "Status of the Thirty Meter Telescope site selection program", SPIE 7012-68, Marseille, France, (2008).

[8] Dalrymple, N.E., "ATST Primary Mirror Thermal Analysis: Zero-Dimensional, Time-Dependent Model", ATST Project, April, (2002).

[9] Cho, M., Corredor, A., Vogiatzis, K., and Angeli, G. "Thermal Performance Prediction of the TMT Optics, SPIE 7017-43, Marseille, France, (2008).